***The following resources related to this article are available online at
www.sciencemag.org (this information is current as of October 8, 2014):***

Updated information and services, including high-resolution figures, can be found in the online version of this article at:
http://www.sciencemag.org/content/335/6073/1184

Supporting Online Material can be found at:
http://www.sciencemag.org/content/suppl/2012/03/08/335.6073.1184.DC1.html

A list of selected additional articles on the Science Web sites **related to this article** can be found at:
http://www.sciencemag.org/content/335/6073/1184#related

This article **cites 30 articles**, 5 of which can be accessed free:
http://www.sciencemag.org/content/335/6073/1184#ref-list-1

This article has been **cited by** 2 articles hosted by HighWire Press; see:
http://www.sciencemag.org/content/335/6073/1184#related-urls

This article appears in the following **subject collections:**
Engineering
http://www.sciencemag.org/cgi/collection/engineering
Geochemistry, Geophysics
http://www.sciencemag.org/cgi/collection/geochem_phys

Nuclear Fuel in a Reactor Accident

Peter C. Burns,[1]* Rodney C. Ewing,[2] Alexandra Navrotsky[3]

Nuclear accidents that lead to melting of a reactor core create heterogeneous materials containing hundreds of radionuclides, many with short half-lives. The long-lived fission products and transuranium elements within damaged fuel remain a concern for millennia. Currently, accurate fundamental models for the prediction of release rates of radionuclides from fuel, especially in contact with water, after an accident remain limited. Relatively little is known about fuel corrosion and radionuclide release under the extreme chemical, radiation, and thermal conditions during and subsequent to a nuclear accident. We review the current understanding of nuclear fuel interactions with the environment, including studies over the relatively narrow range of geochemical, hydrological, and radiation environments relevant to geological repository performance, and discuss priorities for research needed to develop future predictive models.

Nuclear fuels are designed to perform under the extreme but well-defined conditions of a nuclear reactor operating normally. UO_2, used in most commercial power plants, is a suitable fuel in part because of its high melting point (2865°C) and high thermal conductivity. Fresh (unirradiated) UO_2 fuel is modestly radioactive and chemically pure, whereas irradiated (used) fuel is chemically complex and extremely radioactive. During reactor operation, the composition of the fuel gradually changes as ^{235}U is fissioned and transuranium elements (Np, Pu, and higher actinides) form through neutron capture by ^{238}U and subsequent β-decay. The UO_2 fuel retains many of the generated transuranium elements and some fission products within its structure, whereas other radionuclides form new oxide phases, are trapped as gases in bubbles, or segregate as metallic inclusions. Due to the long-term risks associated with transportation, storage, and disposal of used fuel, studies have examined the interaction of irradiated UO_2 fuels with the geochemical and hydrologic environments of potential geological repositories. Such interactions will occur over tens to hundreds of thousands of years, during which time the thermal and radiation fields diminish substantially (1–3). However, much less attention has focused on irradiated fuel and its interaction with the environment during and after an accident at an operating nuclear reactor. Conditions in such events are often unanticipated, and a substantial amount of potentially harmful radioactive material can be released just at the time when the thermal output and level of radioactivity are highest. Furthermore, explosions and melting of fuel and of reactor structural and containment materials slow the accident response, and the movement and redistribution of fuel and moderators create the added concern of continued or sporadic criticality. Months to years may pass before remotely controlled instruments can reveal the final condition and configuration of the fuel. An understanding of how damaged fuel will interact with local, rapidly changing conditions is essential to reduce the potential release of radionuclides.
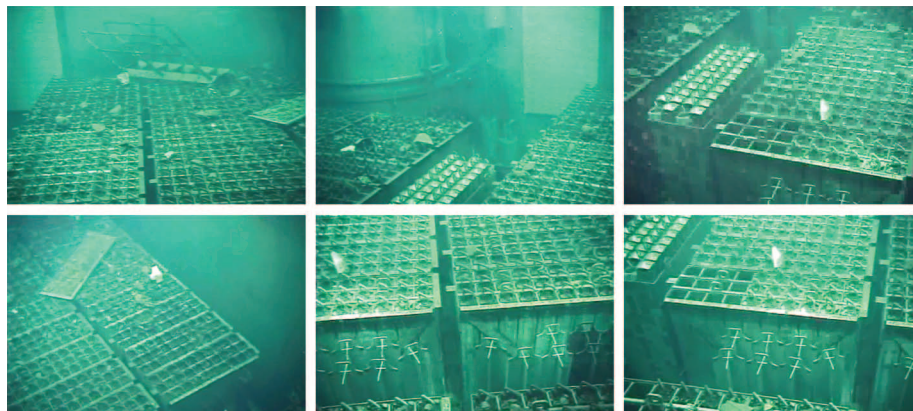
What Happens During a Nuclear Core-Melt Accident?

A core-melt accident occurs when cooling capacity is lost in an operating or recently shut-down nuclear reactor and melting of the reactor core, including nuclear fuels, ensues. Even after stopping fission of uranium in a fuel by insertion of neutron-absorbing control rods, tremendous amounts of heat generated by radioactive decay must be removed to prevent the core from melting. Such core-melt events have not been particularly rare. The first occurred in the early 1950s, with about 20 having occurred worldwide in military and commercial reactors. Some of these had negligible environmental impact, but little information is available concerning some of the events that took place in the former Soviet Union and/or on their nuclear-powered submarines. The most recent and dramatic incidents occurred at operating commercial nuclear power plants: Three Mile Island, USA (1979); Chernobyl, USSR (1986); and Fukushima, Japan (2011) (Fig. 1). Each was very different in its scale and the conditions experienced by the fuel during and after the accident.

At Three Mile Island, a single pressurized water reactor core was partially melted after interruption of cooling. Approximately half of the core was damaged or melted; some 20 metric tons of melted fuel and structural materials flowed to the bottom of the pressure vessel (4). The remaining fuel was damaged by the failure of about 90% of the fuel cladding. Radioactive fission product gases were released from primary containment by venting, but there was no dispersion of particulates of the fuel, and most fission products and transuranium elements were contained within the facility (4).

In contrast to the containment of radioactivity at Three Mile Island, the accident at Chernobyl resulted in the explosive release of radioactive material (5). Steam explosions and burning graphite destroyed the graphite-moderated reactor. Fission gases (e.g., Kr and Xe) and volatile fission products (e.g., I and Cs) were released. Explosions caused the dispersal of about 6 tons of fuel as air-borne particles. Most of the core, about 190 tons, was damaged or melted. The formation of "lava" consisting of melted fuel assemblies, structural materials such as concrete and steel, and sand, lead, and boric acid, added to control criticality and reduce the release of radionuclides, is a remarkable feature of the Chernobyl event. The "lava" moved to the lower levels of the reactor, forming "flows" with an estimated mass of tens of metric tons. Unusual actinide phases, such as a high-uranium zircon ($U_xZr_{1-x}SiO_4$), formed in this solidified melt (6).

The accident at Fukushima Daiichi in Japan, following the magnitude 9.0 Tohoku-oki earthquake and subsequent tsunami on 11 March 2011, occurred while only three (units 1, 2, and 3) of six boiling water reactors were in operation. Most

[1]Department of Civil Engineering and Geological Sciences, and Department of Chemistry and Biochemistry, University of Notre Dame, 156 Fitzpatrick Hall, Notre Dame, IN 46556, USA. [2]Department of Earth and Environmental Sciences, and Department of Nuclear Engineering and Radiological Sciences, University of Michigan, Ann Arbor, MI 48109, USA. [3]Peter A. Rock Thermochemistry Laboratory, University of California, Davis, One Shields Avenue, Davis, CA 95616, USA.

*To whom correspondence should be addressed. E-mail: pburns@nd.edu

Fig. 1. Images extracted from a video posted 8 May 2011 by TEPCO entitled "Status of the spent fuel pool of unit 4 of Fukushima Daiichi nuclear power station." These images, obtained by an underwater robotic camera, show used fuel assemblies and debris in the pool.
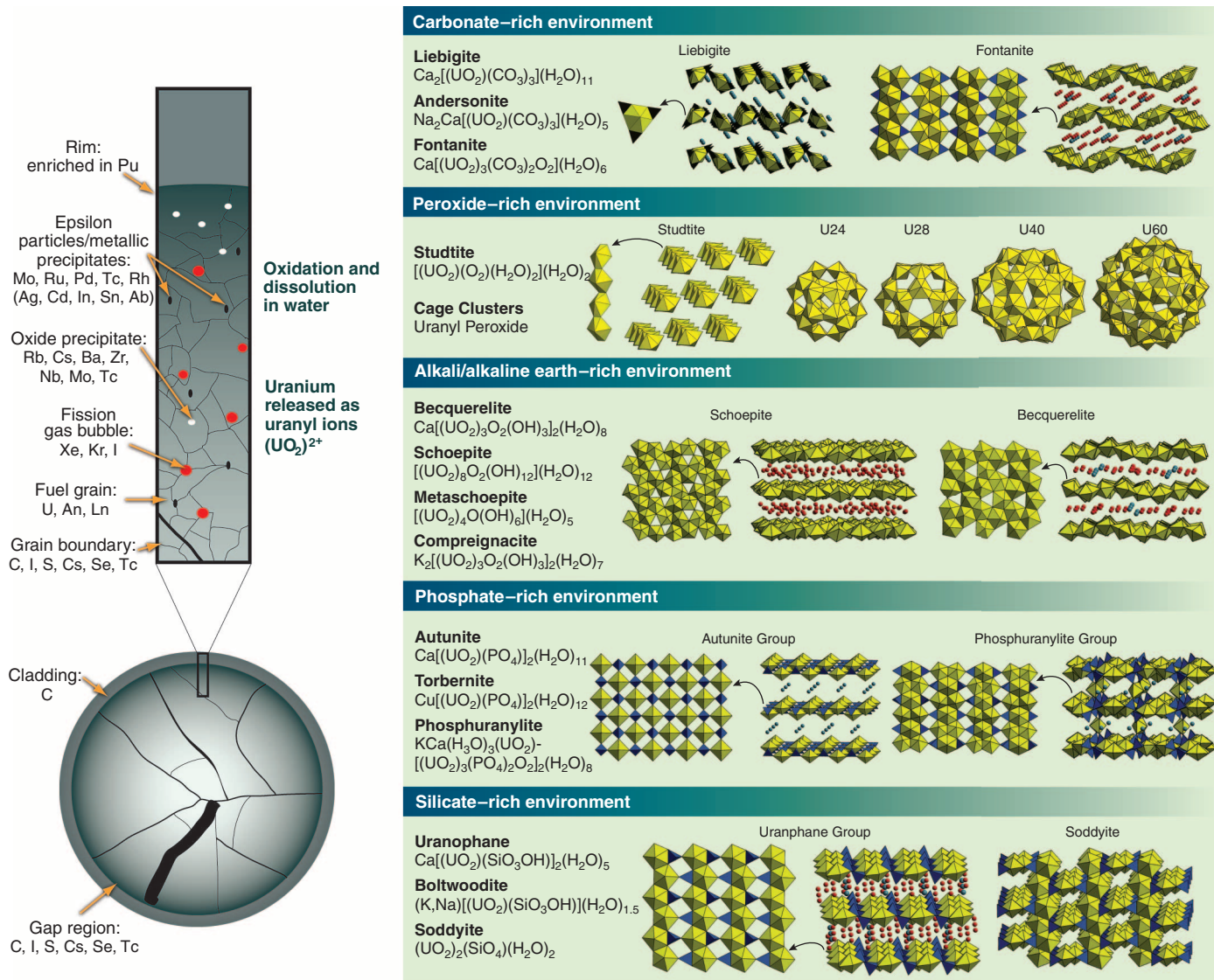
Fig. 2. A schematic representation of irradiated UO$_2$ fuel [left, adapted from (2)] and the structures of various uranyl minerals and nanoscale clusters (right). A cross-section of the 10-mm-wide fuel element and its zirconium alloy cladding is shown, where heat-induced cracks are evident. An expanded view of the fuel and cladding near its edge illustrates that fission products concentrate at grain boundaries, in epsilon phase metallic precipitates, and in gaseous bubbles. Actinides and lanthanides are in the UO$_2$ structure. For the structure representations (35, 39), uranyl polyhedra are shown in yellow, and O atoms are illustrated as red balls.

of the fuel in these reactors was UO$_2$, although there were also 32 mixed-oxide fuel assemblies containing ~6% Pu in unit 3, corresponding to ~4% of the core loading. The operating units shut down promptly in response to the earthquake; however, when the tsunami inundated the site about 40 min later, electrical power was lost, followed by the loss of on-site backup power, resulting in a station blackout and a loss of reactor coolant. A partial core-melt event ensued in units 1, 2, and 3. In a preliminary analysis, the Japanese operator TEPCO has surmised that there was a nearly immediate loss of core cooling in unit 1 and almost all of the fuel assemblies melted and accumulated in the bottom of the pressure vessel. Partial melting of the cores in units 2 and 3, damaging approximately one-third of the fuel assemblies in each, occurred over the following days. Reaction of the zirco-nium alloy (Zircaloy) fuel cladding with water at high temperatures generated hydrogen gas that accumulated and exploded in four of the units. Seawater was injected into the three active reactors and sprayed onto fuel storage pools (e.g., near unit 4) to cool them (Fig. 1). With boiling and evaporation of seawater, large amounts of salt may have deposited in the reactor cores. The release of radioactivity other than gaseous and volatile fission products at Fukushima Daiichi, unlike at Chernobyl, was dominated by the many metric tons of seawater used to cool the cores and storage pools. An unknown fraction of this water was released to the environment, together with accumulation in the basements and trenches of the reactors. Direct discharge of contaminated water to the ocean and groundwater occurred through approximately 8 April 2011 (7). Estimates of the amount of radioactivity released differ by a factor of about 20, with one of the higher estimates indicating that 27,000 terabecquerels of ^{137}Cs was discharged to the ocean (8).

What Types of Radioactive Materials Are Released from Damaged Nuclear Fuel?

Fresh (unirradiated) light water reactor fuel typically consists of UO$_2$ with 1 to 5 atomic percent fissile ^{235}U. When such fuel is removed from a reactor, its radioactivity is 10^{17} becquerel/metric ton, about a factor of a million higher than that of fresh fuel. A year later, the dose rate 1 m from a fuel assembly is about 1 million millisieverts (mSv) per hour (natural background ≈ 3 mSv/year), which will give a lethal dose to a human in less than a minute. The bulk of the penetrating β and γ ionizing radiation arises from short-lived fission products (e.g., ^{131}I, ^{137}Cs, ^{90}Sr) and activation products of components of the fuel assemblies

(e.g., Co, Ni, Nb). Alpha radiation is mostly from the transuranium elements (e.g., [239]Pu, [237]Np, [241]Am), some of which are long-lived (e.g., [239]Pu and [237]Np with half-lives of 24,100 and 2.1 million years, respectively). After about 10,000 years, the total activity of fuel is less than 0.01% of the activity a year after removal from the reactor (9). Tremendous heat is generated by radioactive decay initially, about 2 MW per ton immediately after removal from the reactor, declining to about 20,000 W per ton after a year (10).

Irradiated UO_2 fuels, the details of which are important for reactor operation and potential disposal in a geological repository (11, 12), consist of more than 95% UO_2. The complex mixture of other components within the fuel assembly depends on the conditions of reactor operation (Fig. 2) (13). Gaseous fission products (e.g., Xe and Kr) are present as finely dispersed bubbles within fuel grains (14). Metallic fission products (e.g., Mo, Tc, Ru, Rh, Pd) are dispersed in the fuel as micrometer- or nanometer-sized immiscible particles (14). Other fission products occur as oxide precipitates (e.g., Rb, Cs, Ba, Zr) or in solid solution within the UO_2 fuel matrix (e.g., Sr, Zr, Nb, and lanthanides) (14). Transuranium elements are in solid solution within the UO_2 matrix (e.g., Np, Pu, Am) (14). The steep thermal gradient present in a single fuel pellet during reactor operation, from 400°C at the rim to 1700°C in the center, causes grain coarsening and microfracturing and ensures that the distribution of radionuclides is heterogeneous (14). Volatile elements (e.g., Cs, I) migrate into grain boundaries and fractures within the fuel, as well as into the "gap" between the edges of the fuel pellet and the surrounding metal cladding (14). Non-uniform burn-up in a fuel pellet gives higher concentrations of [239]Pu near the pellet edge, an increase in porosity, polygonization of the UO_2 grains, and a reduction in the size of individual grains (~0.15 to 0.3 μm) (13).

Several experiments in the United States, France, Canada, and Japan give considerable insight into the progression of core-melt incidents and release of fission products from damaged fuel (14–17). Stages occur as temperature increases (17): melting of the Ag-In-Cd absorber alloy at 800°C; deformation and bursting of fuel cladding at 750° to 1100°C; steam oxidation of structural and fuel rod materials beginning at 1200°C; eutectic interactions of cladding with stainless steel beginning at 1300°C; melting of stainless steel by 1450°C and interactions of cladding with UO_2 fuel by 1500°C; melting of cladding at 1760°C; partial reduction of UO_2 due to interactions with cladding and partial dissolution of the fuel and formation of a Zr-U-O melt above 1760°C; and melting of ZrO_2 at 2690°C and UO_2 at 2850°C. Studies of irradiated fuel to temperatures as high as 2530°C indicate release fractions of ~90% for cesium, iodine, and noble gas fission products; up to 50% for molybdenum; less than 1% for strontium; and very low release of actinides (14). Release

of volatile fission products to the atmosphere can occur as soon as the fuel assembly is damaged. These contribute greatly to the shorter-term environmental impact because of the penetrating ionizing radiation they produce and their mobility in air and water. After the initial release of gaseous and volatile radionuclides from damaged fuel assemblies, and in the absence of subsequent explosions that disperse radioactive material such as at Chernobyl, the major potential pathway for continued release of radionuclides is through flowing water.

How Does Water Interact with Irradiated Fuel?

Many radionuclides form aqueous complexes that are soluble in water. Furthermore, water promotes dissolution of the rod/fuel matrix, which releases radionuclides trapped within the matrix (3, 10, 18, 19). Some of these radionuclides have long half-lives (10^3 to 10^6 years) and pose a much longer environmental hazard than the short-lived gaseous and volatile fission products with half-lives of minutes to a few years. Several of the longer-lived radionuclides of concern are redox active (e.g., isotopes of Tc, Se, Np, Pu), and their concentration in water depends strongly on oxidation state, with solid phases with higher oxidation state typically having higher solubility. Exposure to air is sufficient to oxidize some of these cations, albeit slowly under ambient conditions. The radiolytic breakdown of water creates oxidants (e.g., hydrogen peroxide) that can accelerate the oxidative corrosion of fuel (19–23).

Under oxidizing conditions, UO_2 fuel dissolves in aqueous solution by oxidation to uranyl $(UO_2)^{2+}$ ions (10). The uranyl cation is readily complexed by inorganic and organic species (10). The concentration of uranyl in aqueous systems is strongly influenced by complexing species, such as peroxide, carbonate, or nitrate, which greatly enhance solubility, or phosphate, silica, or vanadate, which reduce solubility (24). Complexation effects can be pH dependent. Uranyl peroxide species that are insoluble under acidic conditions are highly soluble in alkaline solutions, and carbonate complexes the uranyl ion

only under alkaline conditions (25). The mobility of dissolved uranyl cations can be diminished by adsorption of uranium onto mineral surfaces (26) and by reduction to less soluble U(IV) by microbial activity (27).

Secondary solid uranyl alteration phases that can form subsequent to water contacting irradiated fuel depend on the amount of water present, the flow rate, the intensity of the radiation field, the availability of species in the water that can complex metals, and redox reactions. On cooled Chernobyl "lava" exposed to water, two secondary phases have been identified: $Na_4(UO_2)(CO_3)_3$ and studtite $[(UO_2)(O_2)(H_2O)_2(H_2O)_2]$ (28). Studtite incorporates peroxide from the radiolytic decomposition of water and suggests local highly oxidizing conditions. Studtite has been reported as a major alteration phase of fuel-element claddings underwater in a cooling pond (29). Studtite also forms on spent fuel in deionized water under laboratory conditions (19) and on UO_2 doped with alpha emitters or irradiated by an external source in water (21–23).

Interaction of irradiated fuel with groundwater can lead to the formation of secondary uranyl minerals (Fig. 2) (3, 10, 18). In general, the long-term fate of uranium released to the environment from dissolving fuel is dispersal or formation of mineral phases that are generally similar to those from which the uranium was initially mined. Combining water and irradiated UO_2 can result in uranyl oxyhydrate minerals, such as schoepite and studtite (Fig. 2). If silica, vanadate, or phosphate are in solution, uranyl minerals such as autunite, carnotite, or uranophane may form. The specific uranyl compounds that precipitate are heavily influenced by the cations and anions available in the aqueous solution—for example, Na and K in the case of seawater (30).

Uranyl minerals can reduce the mobility of key radionuclides, analogous to the role of the original UO_2 fuel in retaining radionuclides within its matrix. Uranyl minerals can incorporate radionuclides into their structures as major constituents (Cs, Sr) or by substitution at the U sites (Pu, Np) (31, 32), and the details of their struc-
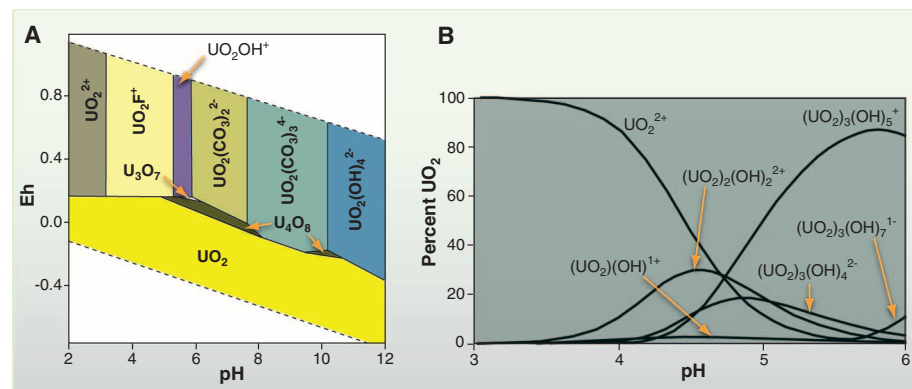
Fig. 3. Examples of stability diagrams for uranium systems. (**A**) Speciation of uranium in a hypothetical groundwater at 25°C [adapted from (8)]. (**B**) Speciation of U(VI) versus pH in NaCl solution at 25°C, concentration of UO_2 = 0.001 M, I = 0.5 M [adapted from (40)].

tures dictate the extent of incorporation. The solubility and stability of uranyl minerals with incorporated radionuclides are important factors in determining the long-term environmental impact of fuel dissolution. There has been substantial improvement in the thermodynamic database for such minerals over the past decade (33), so it is, in principle, possible to calculate the equilibrium phase diagrams for aqueous uranyl systems as a function of pH and the concentrations of various cations and anions (Fig. 3). Much of the remaining uncertainty in such calculations arises from poorly known activity coefficients of uranium species in aqueous solution, especially above room temperature. This uncertainty increases with increasing concentrations of other species in the aqueous phase. Most studies have focused on the reactions of nuclear fuel in groundwater, which is very dilute compared to the seawater to which the Fukushima Daiichi fuel was exposed. The uncertainty also increases with rising temperature because of large uncertainties in the thermodynamic properties of aqueous species at elevated temperatures.

Peroxide produced by radiolysis of water increases the dissolution rate of fuel by oxidizing U(IV) to U(VI) (19–23). If the aqueous system is acidic to neutral and contains low concentrations of complexing agents other than peroxide, studtite will precipitate once peroxide levels are high enough, as seen in laboratory experiments (19) and on stored fuel elements (29). Thermochemical measurements have shown that, although studtite is not stable in the absence of peroxide, it is stabilized by the low concentrations of peroxide produced by radiolysis even in natural uranium deposits, and its formation at the fuel-water interface is thermodynamically reasonable (34). If the water is alkaline, soluble nanoscale uranyl peroxo cage clusters are likely to form and persist in solution (35). Recent studies have identified a large variety of such clusters containing uranyl ions and peroxide groups (Fig. 2). These cage clusters, as well as simpler uranyl peroxo-complexes, form in peroxide-bearing solutions and can crystallize with appropriate charge-balancing alkali ions, including sodium, or remain in aqueous solution for several months or more (36). Calorimetric studies suggest that such alkali uranyl peroxide cluster compounds are energetic intermediates between uranyl species in solution and alkali uranyl minerals when peroxide and alkali ions are present (36). It is unknown whether such alkali uranyl peroxide cluster compounds form under the high-salinity conditions encountered at Fukushima Daiichi, or whether they offer another mechanism for corrosion of fuel and transport and/or precipitation of uranium when seawater is encountered, but this possibility must be considered.

Rates of dissolution of UO_2 in water have been studied under conditions relevant to geological repositories (1, 10, 37), where the aqueous phase is groundwater. Most of these tests followed set protocols that were not optimized to provide fundamental kinetic data that could be modeled and extrapolated to other conditions, such as a reactor accident. There is controversy over whether microbial action substantially increases dissolution rates under certain conditions (38). Thus, at present there is no reliable way of predicting dissolution rates of damaged fuel in water under the conditions of a nuclear accident, especially one like Fukushima Daiichi in which fuel is exposed to hot or boiling seawater for periods of weeks to months. Fukushima Daiichi itself would provide a very instructive experiment if and when it becomes possible to retrieve and study the fuel.

Outlook

Nuclear reactor core-melt accidents are inherently complex and difficult to model, a situation that can be greatly exacerbated by the addition of large quantities of seawater or other materials during and subsequent to the event. Yet, an understanding of the factors that determine radionuclide release is central to taking appropriate and timely action in order to minimize impacts on the environment and human health. Release of volatile and gaseous fission products during a core-melt event is effectively instantaneous, and this contributes dramatically to the near-term environmental impact due to their atmospheric dispersion. Water that interacts with damaged fuel will transport radionuclides that present both short-term and longer-term environmental risk, beginning with the core-melt event and potentially continuing for many years if the damaged fuel is not adequately isolated from the environment. The events at Fukushima Daiichi have demonstrated the importance of water-borne radionuclide transport after a core-melt event, with as much as 27,000 terabecquerels of ^{137}Cs being released to the ocean (8).

At present, there is not an adequate, quantitative understanding of water interactions with damaged fuel, including reaction mechanisms and rates, radionuclide release and transport, and exposure pathways. Resolidified fuel from a core-melt accident is very heterogeneous and has a much more complex phase chemistry than undamaged fuel. Past repository-focused studies of the release of radionuclides from undamaged fuel generally cannot be extrapolated to the extreme conditions of temperature and radiation field that occur during and subsequent to a core-melt event. Central to gaining a predictive understanding is the characterization of resolidified fuel derived from a core-melt event in terms of the distribution and reactivity of radionuclides, the basic phase chemistry, and the resulting microstructure. Some of this information can be obtained by investigating simulated core-melt events with fuel analogs that contain nonradioactive isotopes of the fission products distributed in UO_2. The need to understand the behavior of actinides, for which there are no nonradioactive isotopes, and the effects induced by intense radiation fields require studies using radioactive materials. The role of complexation in mobilizing radionuclides in water at high temperatures, as well as that of nanoscale actinide materials in promoting the dissolution of fuel, must be better understood. Studies outlined here are both difficult and expensive, but are essential to reduce the risk associated with an increasing reliance on nuclear energy. The resulting understanding may also help in the future design of fuel assemblies and reactors that are better able to withstand potential accidents.

References and Notes

1. D. W. Shoesmith, *J. Nucl. Mater.* **282**, 1 (2000).
2. E. C. Buck, B. D. Hanson, B. K. McNamara, in *Energy, Waste, and the Environment: A Geochemical Perspective*, R. Gieré, P. Stille, Eds. (Geological Society of London, Special Publications, London, 2004), vol. 236, pp. 65–88.
3. P. A. Finn, J. C. Hoh, S. F. Wolf, S. A. Slater, J. K. Bates, *Radiochim. Acta* **74**, 65 (1996).
4. M. Rogovin, G. T. Frampton, "Three Mile Island: A report to the commissioners and to the public" (Nuclear Regulatory Commission, Washington, DC, 1980).
5. E. B. Anderson, B. E. Burakov, E. M. Pazukhin, *Soviet Radiochem.* **34**, 632 (1993).
6. E. B. Anderson, B. E. Burakov, E. M. Pazukhin, *Radiochim. Acta* **60**, 149 (1993).
7. K. Buesseler, M. Aoyama, M. Fukasawa, *Environ. Sci. Technol.* **45**, 9931 (2011).
8. "Synthèse actualisée des connaissances relatives à l'impact sur le milieu marin des rejets radioactifs du site nucléaire accidenté de Fukushima Dai-ichi" (Institut de Radioprotection et de Sûreté Nucléaire, 2011).
9. A. Hedin, *Spent Nuclear Fuel—How Dangerous Is It?* (Swedish Nuclear Fuel and Waste Management, Stockholm, 1997).
10. J. Bruno, R. C. Ewing, *Elements* **2**, 343 (2006).
11. L. H. Johnson, D. W. Shoesmith, in *Radioactive Waste Forms for the Future,* W. Lutze, R. C. Ewing, Eds. (North-Holland, Amsterdam, 1988), pp. 635–698.
12. V. M. Oversby, in *Materials Science and Technology*, R. W. Cahn, P. Haasen, E. J. Kramer, Eds. (VCH Verlagsgessellschaft mbH, Germany, 1994), vol. 10B, chap. 12, pp. 391–442.
13. H. Kleykamp, *J. Nucl. Mater.* **131**, 221 (1985).
14. B. J. Lewis, W. T. Thompson, F. C. Iglesias, in *Comprehensive Nuclear Materials*, R. J. M. Konings, Ed. (Elsevier, Amsterdam, 2012), vol. 2, pp. 515–546.
15. T. Fuketa, H. Sasajima, Y. Mori, K. Ishijima, *J. Nucl. Mater.* **248**, 249 (1997).
16. P. Hofmann, *J. Nucl. Mater.* **270**, 194 (1999).
17. B. J. Lewis, R. Dickson, F. C. Iglesias, G. Ducros, T. Kudo, *J. Nucl. Mater.* **380**, 126 (2008).
18. R. J. Finch, E. C. Buck, P. A. Finn, J. K. Bates, in *Scientific Basis for Nuclear Waste Management XXII*, D. J. Wronkiewicz, J. H. Lee, Eds. (Materials Research Society, Warrendale, PA, 1999), vol. 556, pp. 431–438.
19. B. Hanson et al., *Radiochim. Acta* **93**, 159 (2005).
20. D. Y. Chung et al., *J. Radioanal. Nucl. Chem.* **284**, 123 (2010).
21. F. Clarens et al., *Environ. Sci. Technol.* **38**, 6656 (2004).
22. C. Corbel et al., *J. Nucl. Mater.* **348**, 1 (2006).
23. G. Sattonnay et al., *J. Nucl. Mater.* **288**, 11 (2001).
24. D. Gorman-Lewis, P. C. Burns, J. B. Fein, *J. Chem. Thermodyn.* **40**, 335 (2008).
25. D. L. Clark, D. E. Hobart, M. P. Neu, *Chem. Rev.* **95**, 25 (1995).
26. T. D. Waite, J. A. Davis, T. E. Payne, G. A. Waychunas, N. Xu, *Geochim. Cosmochim. Acta* **58**, 5465 (1994).
27. Y. Suzuki, S. D. Kelly, K. M. Kemner, J. F. Banfield, *Nature* **419**, 134 (2002).
28. B. E. Burakov, E. E. Strykanova, E. B. Anderson, in *Scientific Basis for Nuclear Waste Management XX*, W. J. Gray, I. R. Triay, Eds. (1997), vol. 465, pp. 1309–1311.
29. J. Abrefah, S. Marschmann, E. D. Jenson, "Examination of the surface coatings removed from K-East Basin fuel elements" (PNNL-11806, Pacific Northwest National Laboratory, Richland, WA, 1998).
30. R. J. Finch, R. C. Ewing, *J. Nucl. Mater.* **190**, 133 (1992).

31. P. C. Burns, P. C. Ewing, M. L. Miller, *J. Nucl. Mater.* **245**, 1 (1997).
32. M. Douglas *et al.*, *Environ. Sci. Technol.* **39**, 4117 (2005).
33. T. Y. Shvareva *et al.*, *Geochim. Cosmochim. Acta* **75**, 5269 (2011).
34. K. A. H. Kubatko, K. B. Helean, A. Navrotsky, P. C. Burns, *Science* **302**, 1191 (2003).
35. P. C. Burns, *Min. Mag. (London)* **75**, 1 (2011).
36. F. A. Armstrong, J. Hirst, *Proc. Natl. Acad. Sci. U.S.A.* **108**, 14049 (2011).
37. D. W. Shoesmith, S. Sunder, *J. Nucl. Mater.* **190**, 20 (1992).
38. A. Johnsson, A. Odegaard-Jensen, G. Skarnemark, K. Pedersen, *J. Radioanal. Nucl. Chem.* **279**, 619 (2009).
39. P. C. Burns, *Can. Mineral.* **43**, 1839 (2005).
40. A. Gianguzza, D. Milea, F. J. Millero, S. Sammartano, *Mar. Chem.* **85**, 103 (2004).

Natural SIV Hosts: Showing AIDS the Door

Ann Chahroudi,[1,3] Steven E. Bosinger,[3] Thomas H. Vanderford,[3] Mirko Paiardini,[2,3]* Guido Silvestri[2,3]*

Many species of African nonhuman primates are naturally infected with simian immunodeficiency viruses (SIVs) in the wild and in captivity. In contrast to HIV-infected humans, these natural SIV hosts typically do not develop AIDS, despite chronic infection with a highly replicating virus. In this Review, we discuss the most recent advances on the mechanisms of protection from disease progression in natural SIV hosts, with emphasis on how they differ from pathogenic HIV/SIV infections of humans and rhesus macaques. These mechanisms include: (i) resolution of immune activation after acute infection, (ii) restricted pattern of target cell infection, and (iii) protection from mother-to-infant transmission. We highlight the areas that should be pursued in future studies, focusing on potential applications for the treatment and prevention of HIV infection.

O ver thousands of years, species-specific strains of simian immunodeficiency virus (SIV) have endemically infected more than 40 species of African nonhuman primates (*1, 2*) that we will refer to as "natural SIV hosts" or simply, "natural hosts" (Box 1). Multiple cross-species transmissions of SIV_{cpz} from chimpanzees and SIV_{smm} from sooty mangabeys (SMs) to humans have resulted in the current epidemics of HIV-1 and HIV-2, respectively (*3*). SIV_{smm} is also the origin of the SIV_{mac} strains that are used to experimentally infect various species of Asian macaques, resulting in a disease called simian AIDS (*4*). In marked contrast to pathogenic HIV infection of humans and SIV_{mac} infection of rhesus macaques (RMs), SIV infections of natural hosts are typically nonpathogenic, despite high levels of virus replication (*5–9*). The only exception is the SIV_{cpz} infection of chimpanzees that is associated with a significant increase in mortality, although not to the levels seen in HIV-1 or SIV_{mac} infections (*10*). Importantly, the benign infection of natural hosts is distinct from the nonprogressive HIV/SIV infections of a rare subset of humans and RMs, called elite controllers, in which the absence of AIDS is at least partly related to the ability of the immune system to suppress virus replication (*11, 12*). Understanding the mechanisms responsible for the AIDS resistance of natural SIV hosts is considered a key priority in contemporary AIDS research, with major implications for HIV prevention and therapy.

What Is the Phenotype of SIV Infection in Natural Hosts?

Two species of natural SIV hosts that have been intensively studied as captive animals, SMs and the African green monkeys (AGMs), are housed in primate centers in the United States and Europe. Limited information is available about other species such as mandrills, drills, suntailed monkeys, and a few others. In this Review, we mainly discuss data generated from SMs and AGMs because relatively little is known about the phenotype of SIV infection in other natural SIV host species. Given the many similarities of these two models, we discuss them together unless otherwise noted in specific instances. Table 1 shows the main virological and immunological aspects of pathogenic and nonpathogenic primate lentivirus infections.
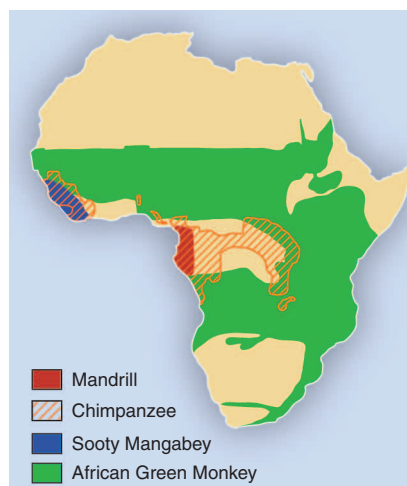
In summary, key similarities between SIV infection of natural hosts and pathogenic HIV/SIV infections of humans and RMs include: (i) high viremia (*5–9*), (ii) short in vivo life span of productively infected cells (*13, 14*), (iii) significant loss of mucosal CD4$^+$ T cells during acute infection (*15, 16*), (iv) high levels of innate and adaptive immune activation during acute infection (*17–21*), and (v) the inability of the host cellular and humoral immune system to control virus replication (*22–24*). This last observation is of great theoretical and practical importance, because it shows that the AIDS resistance of natural SIV hosts is independent of adaptive antiviral immune responses that suppress virus replication. This feature of natural SIV infection highlights the tremendous challenge of artificially inducing, with an AIDS vaccine, a type of protective immunity that has not been selected for in many thousands of years of evolutionary pressure posed by lentiviruses on the nonhuman primate immune system.

Key features of SIV infection that appear to be specific to natural hosts include: (i) preservation of healthy levels of peripheral CD4$^+$ T cells (*5*); (ii) preservation of mucosal immunity and absence of microbial translocation (*16, 25–27*); (iii) normal lymph node architecture and function (*5*); (iv) preservation of T cell regeneration (*28*); (v) preferential sparing of central memory CD4$^+$ T cells (Tcm) from direct virus infection (*29, 30*); and (vi) lack of chronic immune activation (*5, 6, 31–33*). The viral and host factors that contribute to the lack of chronic immune activation and their impact on the benign phenotype of natural SIV infection are depicted in Fig. 1. Another fascinating characteristic of natural SIV infections is the rarity of mother-to-infant-transmission (MTIT) as compared with pathogenic HIV/SIV

[1]Departments of Pediatrics, Emory University School of Medicine, Atlanta, GA, USA. [2]Department of Pathology and Laboratory Medicine, Emory University School of Medicine, Atlanta, GA, USA. [3]Yerkes National Primate Research Center (YNPRC), Emory University, Atlanta, GA, USA.

*To whom correspondence should be addressed. E-mail: gsilves@emory.edu (G.S.); mirko.paiardini@emory.edu (M.P.)

Mandrill
Chimpanzee
Sooty Mangabey
African Green Monkey

Box 1. More than 40 species of African monkeys are endemically infected with a species-specific strain of SIV. Multiple cross-species transmissions of SIV from chimpanzees to humans during the preparation of bush meat, aided by the rise of urbanization in early 20th century Africa, has resulted in the HIV-1 epidemic and all of its subtypes. High rates of mutation, replication, and recombination have fueled the success of these and other zoonotic events, resulting in the generation of the pathogenic lentiviruses, HIV-1, HIV-2, and SIV_{mac} in their respective hosts. The geographic range of selected natural hosts is shown. [Map adapted from (*69*)]